

Measurements of large optical rotary dispersion in the adipose eyelid of Atlantic mackerel (*Scomber scombrus*): Electronic Supplementary Material

Euan Jenkinson, Andrew J. Alexander,^{*} and Philip J. Camp[†]

*School of Chemistry, University of Edinburgh,
David Brewster Road, Edinburgh EH9 3FJ, Scotland*

(Dated: March 6, 2023)

^{*} Corresponding author: andrew.alexander@ed.ac.uk

[†] Corresponding author: philip.camp@ed.ac.uk

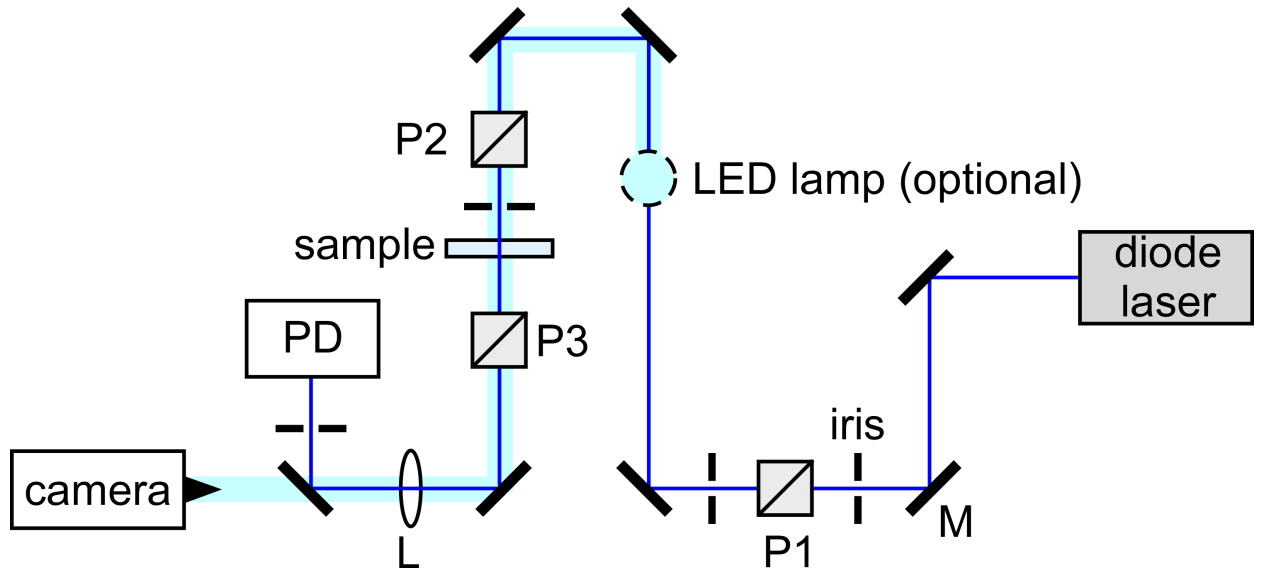


Figure S1. Schematic experimental setup: M = mirror; L = lens; P1-3 = Glan-laser polarizers; PD = photodiode; LED = light-emitting diode. The setup was devised to obviate stress by passing the beam in a vertical direction through the adipose eyelid sample. The beam was steered using a combination of broadband reflective mirrors (M), irises (iris) and a lens (L). A glan-laser polarizer P1 was used to control the power of the beam impinging on the sample and for general cleaning of the polarization; P2 and P3 were the main polarizer and analyser polarizer, respectively. Five different diode lasers were used: 410 nm, 488 nm, 532 nm, 635 nm, and 670 nm; each required realignment due to different beam characteristics, such as diameter and divergence. The intensity of laser light passing through the analyser polarizer was measured using a photodiode (PD). An optional white-light LED lamp could be inserted into the beampath to image the optical rotary dispersion (ORD) using a digital camera (camera). Before making systematic measurements, a mask was placed in front of the sample and positioned to locate a spot that showed good ORD, i.e., a broad range of colours on rotation of the analyser; see figures S3 and S4. The measurement procedure is described in figure S2.

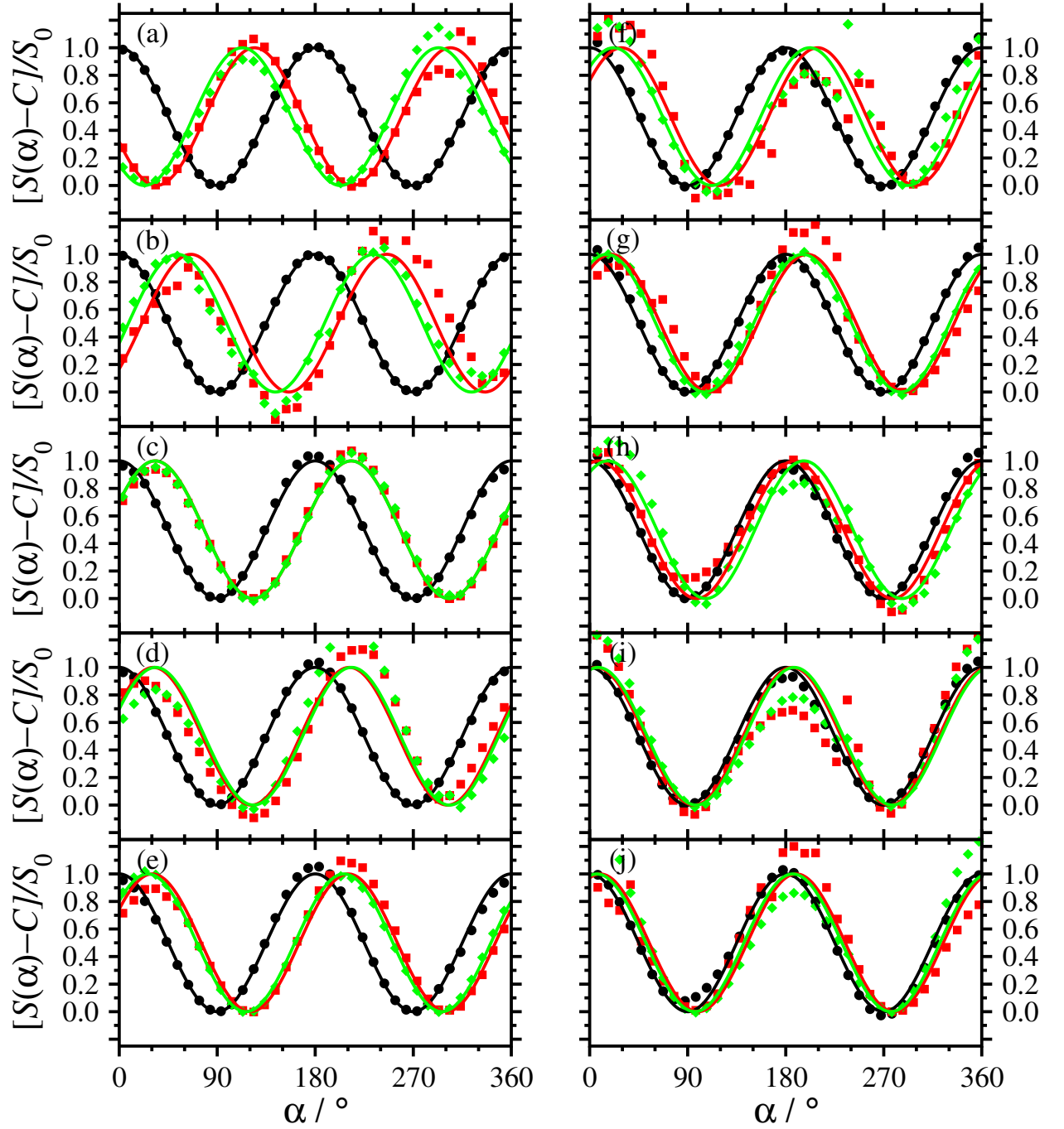


Figure S2. Dependence of the photodiode detector voltage on polarizer angle for sample 1 (a)–(e) and sample 2 (f)–(j): (a) and (f) 410 nm; (b) and (g) 488 nm; (c) and (h) 532 nm; (d) and (i) 635 nm; (e) and (j) 670 nm. In each case, there is one measurement for a blank with no sample in the beam path (black points and black lines), and two measurements for the sample (red and green points). The values of $\theta(\lambda)$ for each measurement were obtained by fitting equation (3.1) from the main text (red and green lines), and then averaged. The resulting values are reported in table 1 of the main text.

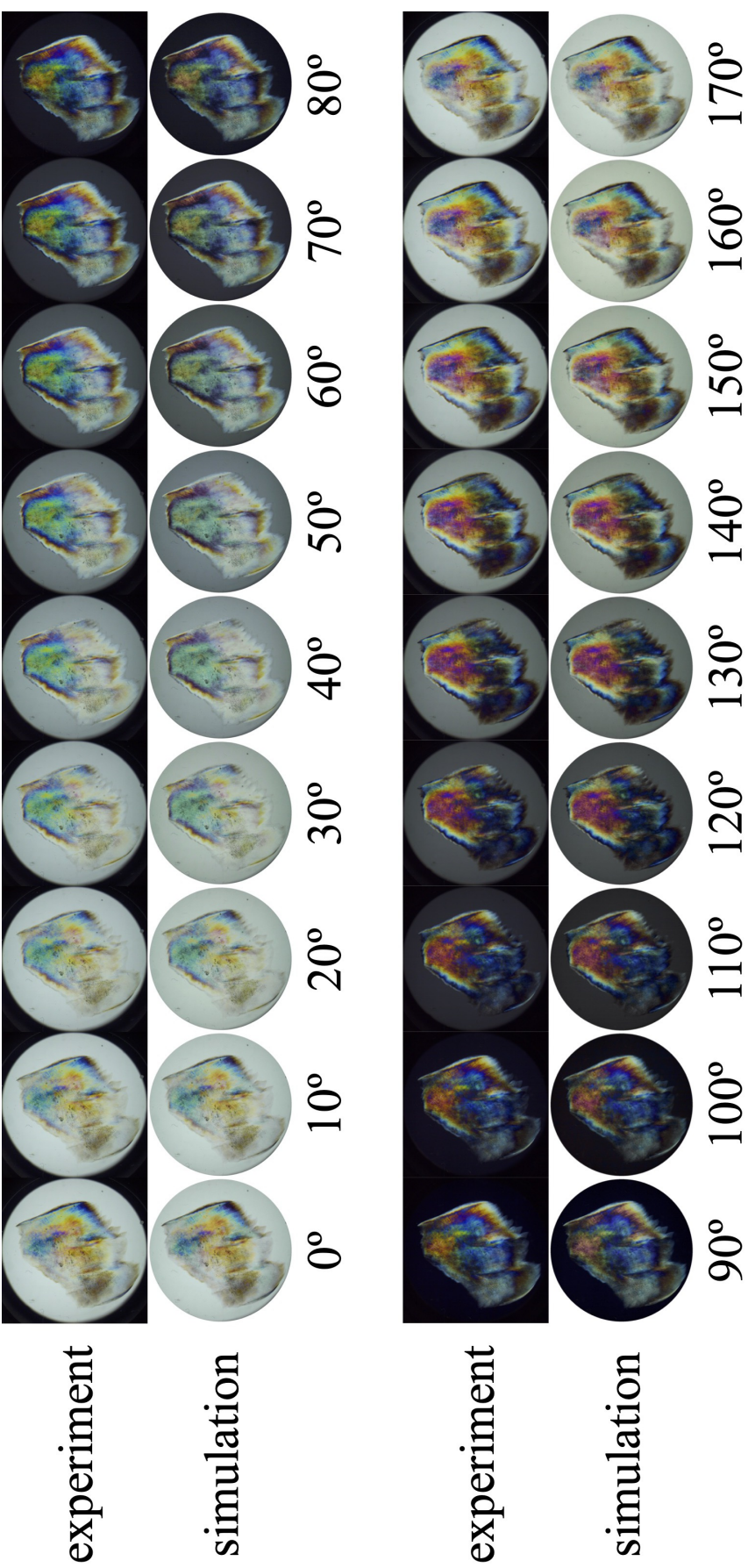


Figure S3. Colour images of sample 1 demonstrating the ORD of adipose eyelid sample from Atlantic mackerel through crossed polarizers as a function of the angle of rotation of the analyzing polarizer. For each polarizer angle, there are two images: 'experiment' is the original image; and 'simulation' is the simulated image.

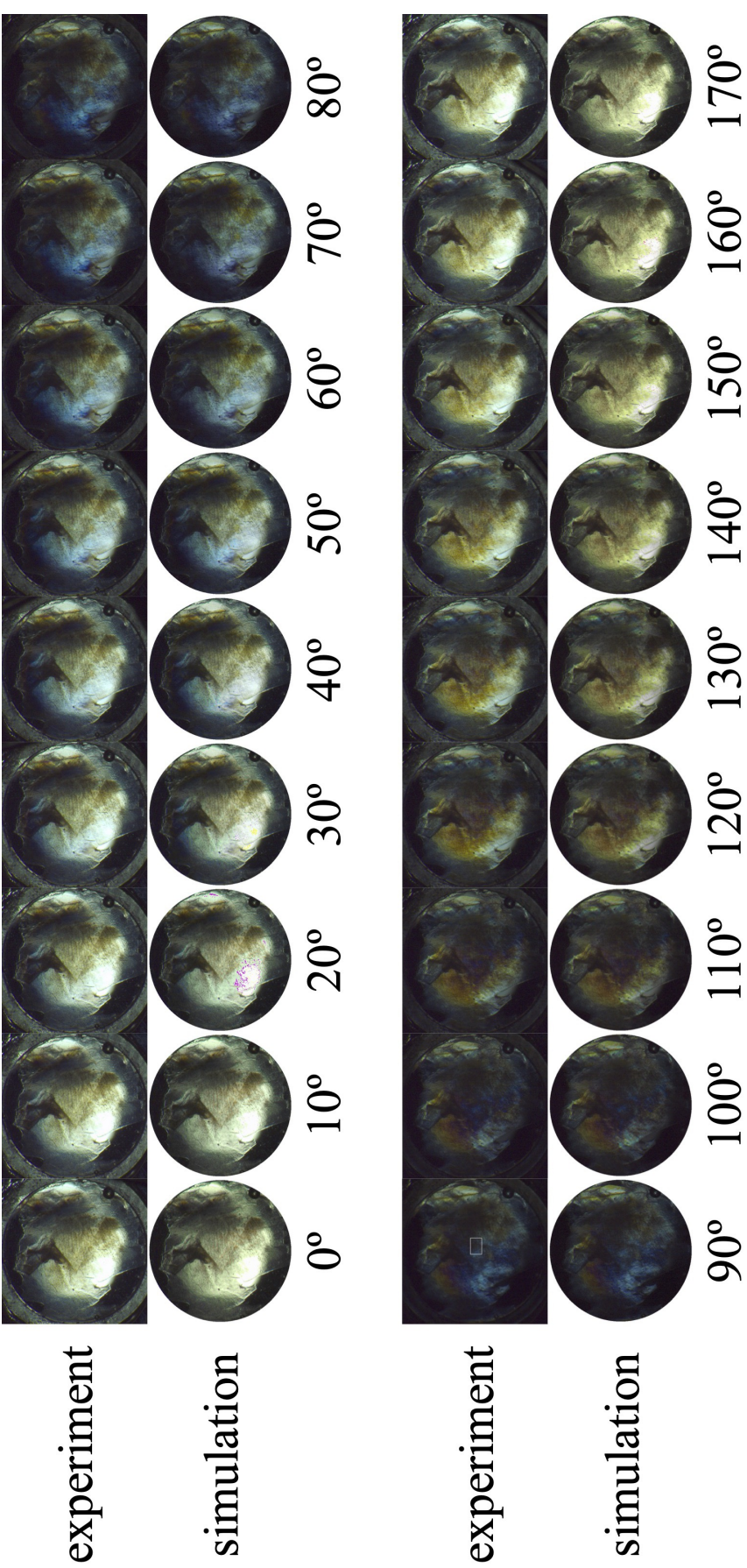


Figure S4. Colour images of sample 2 demonstrating the ORD of adipose eyelid sample from Atlantic mackerel through crossed polarizers as a function of the angle of rotation of the analyzing polarizer. For each polarizer angle, there are two images: 'experiment' is the original image; and 'simulation' is the simulated image. The experimental image for 90° shows the region used subsequently for ORD measurements.

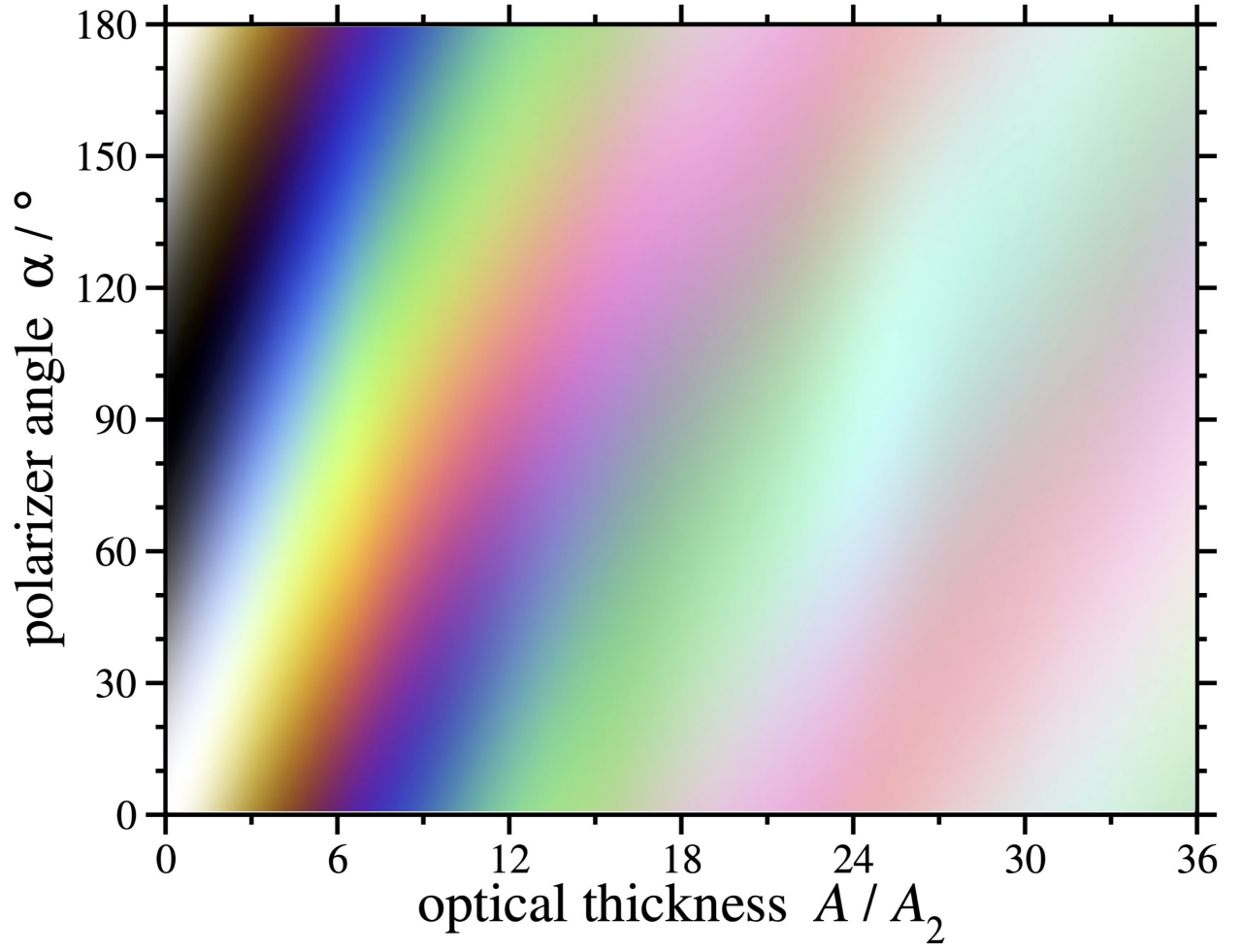


Figure S5. A colour map showing the effect of ORD on incident white light transmitted through a sample with a prescribed optical thickness, expressed in units of A_2 for sample 2 (table 1 of the main text), between polarizers crossed at an angle α .



Figure S6. Average optical-thickness map $A(x, y)$ corresponding to figure S4. The optical thickness is shown on a gray scale, where black corresponds to an optical thickness equal to $A_{\max} = 18A_2$, and white means $A = 0$.